Colloid Polym Sci 277:827–836 (1999)

ORIGINAL CONTRIBUTION

J. Schulte
S. Enders
K. Quitzsch

Rheological studies of aqueous alkylpolyglucoside surfactant solutions

Received: 4 January 1999
Accepted in revised form: 12 April 1999

J. Schulte · S. Enders (✉) · K. Quitzsch
Wilhelm Ostwald Institute of Physical and Theoretical Chemistry
University of Leipzig, Linnestrasse 2
D-04103 Leipzig, Germany

Abstract Alkylpolyglucosides (C_YG_X) are industrial products of mixtures consisting of a hydrocarbon chain with Y carbon atoms linked to X sugar residues. Based on detailed analytical investigation of technical grade alkylpolyglucosides ($C_{8–10}G_X$, $C_{12–14}G_X$ and $C_{8–16}G_X$)/water systems using high-performance liquid chromatography in combination with a special kind of mass spectroscopy their rheological behaviour is discussed and compared to the rheological behaviour of pure alkyl monoglycosides (C_8G_1 and $C_{10}G_1$) in water. The rheological properties that exhibit a dependence on the alkyl chain length, Y, and the degree of polymerisation, X, are investigated by rotation and oscillation experiments over an extended concentration range. The Maxwell model fits the frequency dependence of the dynamic functions fairly well. The viscosity shows an Arrhenius-like dependence on temperature. A comparison is drawn between the monoglucosides and the polyglucosides, which shows that the rheological properties are more sensitive to the a change in chain length than in the degree of polymerisation. Phase transitions, especially liquid-crystalline to isotropic solutions, phase split into two coexisting liquid phases, and could be followed using visual observation and rheology. Depending on the difference in the rheological properties of the corresponding phases, viscoelastic measurements showed these transitions clearly. Additionally, the changes in viscosities were measured after addition of a second surfactant.

Key words Phase equilibria · Surfactant solution · Rheology · Alkylglucosides · Synergism

Introduction

Considering the wide range of applications of surfactant-containing systems, a detailed rheological characterization is quite important for the design of unit operation (pumping, agitation and mixing), quality control and optimization of formulations, establishing relationships with the microstructure. It has been known that such systems can have very complex flow properties, especially viscoelastic properties at high surfactant concentrations [1].

Alkylpolyglucosides (APG) [2, 3, 4], which are widely used as surfactants in commercial products, represent a complex mixture of C_YG_X homologues with different hydrocarbon chain length Y and different number of glucose units X. Although phase diagrams of two technical APG ($C_{8–10}G_X$, $C_{12–14}G_X$ [5, 6, 7]) and pure *n*-alkyl-β-D-glucopyranosides (C_8G_1 [8, 9] and $C_{10}G_1$ [10–14]) in water have been the subject of considerable interest, only a few studies have addressed the rheological properties [5, 12, 15–19]. By combined analysis of dielectric properties and viscosities La Mesa et al. [15]

found a slight and continuous dependence of micellar shape on surfactant content for the C_8G_1/water system. The rheological properties of the pure surfactant systems (C_8G_1/water, $C_{10}G_1$/water), obtained by oscillating measurements, can be described by a simple Maxwell model [12, 18] in the low-frequency range. Micellar aggregation, rheological properties, and phase behaviour of two systems ($C_{8-10}G_X$/water and $C_{12-14}G_X$/water) have been studied [5]. Light-scattering and viscosity experiments show that in water the short-chain $C_{8-10}G_X$ forms spherical micelles up to high surfactant concentrations that are highly hydrated, whereas the long-chain $C_{12-14}G_X$ forms rodlike micelles in water [5]. The isotropic phase of $C_{8-10}G_X$/water which extends to 64 wt% above 298 K is a Newtonian liquid [5]. $C_{12-14}G_X$ solutions are viscoelastic even at low concentrations [5].

Starting from a quantitative analysis of the technical grade products according to their alkyl chain length, Y, and their number of glucose groups, X, the present paper gives a detailed comparison between the rheological properties of the technical grade surfactants ($C_{8-10}G_X$, $C_{12-14}G_X$ and $C_{8-16}G_X$) and two pure *n*-alkyl-β-D-glucopyranosides (C_8G_1, $C_{10}G_1$) [12, 18] in water over a large concentration range.

One method of decreasing the environmental impact of surfactants is to use mixtures of known surfactants that exhibit synergism in their interfacial properties. The requirements, in quantitative terms, for the existence of synergy in mixtures of surfactants have been elucidated for several interfacial phenomena [20, 21]. Shchipunov et al. [17] studied the change in the rheological properties by adding sugar surfactants to lecithin organogels, which consist of extended cylindrical lecithin micelles in an organic nonpolar solvent. However, to date, there has been relatively little work on the rheological properties [17] of surfactant mixtures containing sugar surfactants. In a way, this is very unfortunate because in many practical applications of such systems these properties are of fundamental importance. In this paper we direct our attention to the influence on the viscosity of adding a second surfactant to an aqueous APG solution.

Experimental

Materials

The *n*-octyl-β-D-glucopyranoside (C_8G_1) and *n*-decyl-β-D-glucopyranoside ($C_{10}G_1$) were purchased from Sigma Chemical Co. (USA), and were used without recrystallization. The water was double distilled over potassium permanganate. The technical grade alkylpolyglucosides ($C_{8-10}G_X$, $C_{12-14}G_X$ and $C_{8-16}G_X$) were gifts from Henkel, Düsseldorf, Germany. The other surfactants were supplied by the following companies: Aldrich Chemie (tetramethylbutylphenol pentaethylene glycol ether [Igepal]), Merck, Darmstadt (sodium dodecylsulfate [SDS], Henkel (sodium tetradecylsulfate, sodium hexadecylsulfate and sodium octadecylsulfate [SOS]), Fluka (polyoxyethylene lauryl ether [Brij35]) and Ventron (dodecyl trimethylammonium bromide [DMAB]).

Methods

Rheological measurements

The rheological properties were determined by means of a stress-controlled rotational rheometer, Paar Physica LS100 low-stress rheometer, using a cone-plate measuring system (gap 50 μm, CP50/1 [cone angle 1°, cone radius 50 mm] or CP20/0.5 [cone angle 0.5°, cone radius 20 mm]). The experiments were carried out both at oscillating and constant stress. Care was taken to avoid evaporation. This was achieved by tightly enclosing the measurement system with a solvent trap and saturating the air in the system with water. The frequency range investigated was $0.001\ \text{Hz} \le f \le 15\ \text{Hz}$. A Peltier system provided temperature control with an accuracy of ± 0.1 K.

The rheological properties can be investigated if dynamic experiments are performed [22, 23]. From the phase angle between the stress and the strain and the amplitude of these quantities, the storage modulus, G', the loss modulus G'', and the magnitude of the complex viscosity, $|\eta^*|$, can be calculated. The simplest mechanical model that can describe the dynamic behaviour of a viscoelastic surfactant solution is called a Maxwell material. It consists of a spring and a dashpot connected in series. The behaviour of the Maxwell model under harmonic oscillations can be obtained from the following:

$$G'(\omega) = \frac{G_0\omega^2\tau^2}{1+\omega^2\tau^2} \quad (1)$$

$$G''(\omega) = \frac{G_0\omega\tau}{1+\omega^2\tau^2} \quad (2)$$

$$|\eta^*| = \frac{\eta_0}{\sqrt{1+\omega^2\tau^2}} \quad (3)$$

where ω is the angular frequency, G_0 the zero-shear modulus, η_0 the zero-shear viscosity and τ the structure relaxation time.

High-performance liquid chromatography (HPLC)

The samples were diluted with eluant and injected into a conventional HPLC apparatus provided by Bischoff, Germany. The analysing system consists of an RP-18 column and a 75 wt% methanol/water eluant. The signal was detected refractometrically.

Atmospheric pressure ionization – mass spectroscopy (API-MS)

The experiments were carried out at the University of Leipzig, Institute of Analytical Chemistry, using a Perkin Elmer Sciex API 100 LC/MS system. The experimental conditions were as follows: orifice voltage 100 V and ring voltage 400 V. The eluant was 75 wt% methanol/water with a flow velocity of 0.6 ml/min.

Results and discussion

Characterization of the systems

Analytical composition of the technical grade surfactants

The technical grade surfactants are often synthesised from the corresponding long-chain alcohols. To produce such components on an industrial scale, mixtures of alcohols can be used and purification of the alkylglycosides obtained is difficult because their chromatographic

separation in a normal-phase system is very poor, depending on the chain length [24]. Using reversed-phase HPLC allows the separation of the technical grade surfactant according to the chain length of the hydrophobic tail [2, 25]. Additionally, by-products and unreacted educts can be detected in the HPLC chromatogram. The HPLC chromatograms of three samples are depicted in Fig. 1. The identification of the peaks for water and for surfactant molecules with an alkyl chain length of 8 and 10 took place according to the retention time under identical chromatographic conditions as given in the literature [12, 26]. The retention time for $C_{12}G_1$ was estimated in a separate experiment. The peak at a retention time of 17 min was assigned to a surfactant with a chain length of 14 and the peak at 40 min to molecules with a chain length of 16. Plotting the alkyl chain length versus the logarithm of the retention time gives a straight line. $C_{8-10}G_X$ (Fig. 1A) and $C_{12-14}G_X$ (Fig. 1B) consist mainly of molecules with two different tail lengths. The peak for dodecylglucoside (Fig. 1B) splits into two parts. The reason, therefore, can be the superposition of separation according to the number of glucose groups. The chromatogram for $C_{8-16}G_X$ (Fig. 1C) shows a lot of peaks at different retention times. The peak for a chain length of 12 carbon atoms splits again into two parts.

The results for the technical grade surfactants obtained using API-MS are shown in Fig. 2. This method permits fractionation according to the number of the glucose groups, X, for each molecule differing in the alkyl chain length, Y. The main part of the technical grade surfactant mixtures consist of molecules with one or two glucose groups. The number of molecules with six or more glucose groups is close to the detection limit. In agreement with the HPLC chromatogram $C_{8-10}G_X$ (Fig. 2A) consist mainly of octyl- and decylglucoside. The small amount of tetradecylglucoside (Fig. 1A) was not detectable using API-MS. The number of glucose groups amounts to 2 or 3. $C_{12-14}G_X$ (Fig. 2A) contain dodecyl- and tetradecylglucoside with an average number of glucose groups of 2. In the case of $C_{8-16}G_X$ the small amount of octylglucoside (Fig. 1C) is not detectable using API-MS. Hexadecyl- and decylglucoside (Fig. 2C) mainly have three or four glucose groups. Dodecyl- and tetradecylglucosides are predominantly connected with two glucose groups. The analytical results obtained from HPLC and API-MS measurements are compiled in Table 1. All the following concentrations refer to the real surfactant content and the amount of water is according to Table 1.

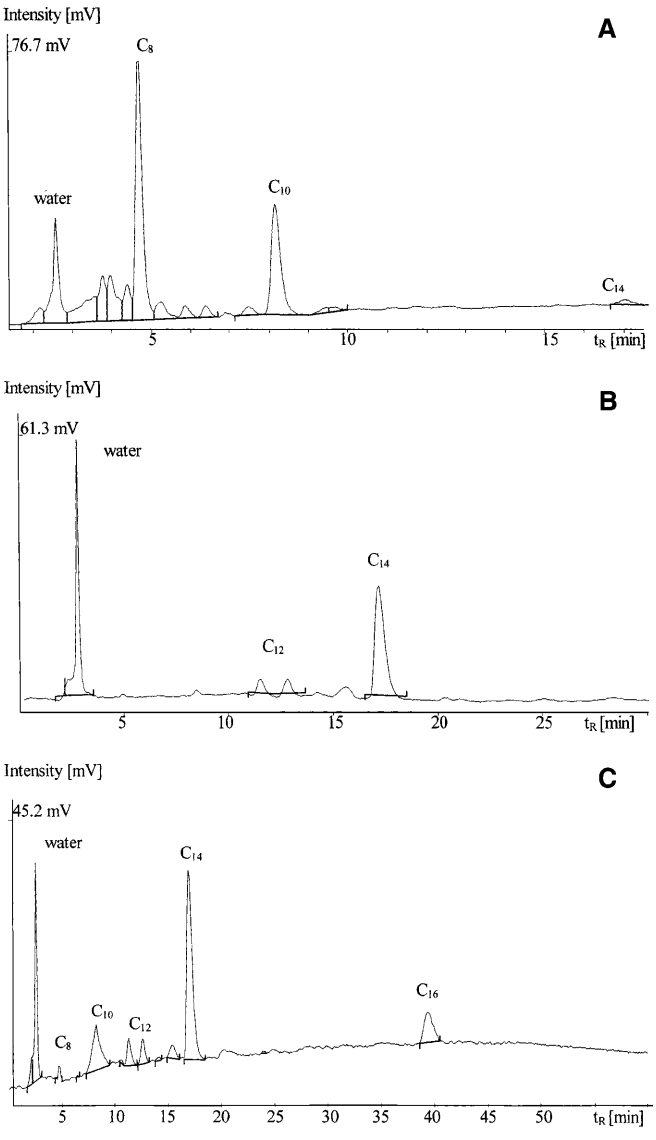

Fig. 1 Chromatogram of **A** $C_{8-10}G_X$, **B** $C_{12-14}G_X$ and **C** $C_{8-16}G_X$

Table 1 Analytical characterization of the technical grade surfactants

Property	$C_{8-10}G_X$	$C_{12-14}G_X$	$C_{8-16}G_X$
Water content (wt%)	35	50	53.5
Weight-average number of the glucose groups	2.46	2	2.47
Weight-average chain length	8.7	13.6	13.2

Phase diagram of the $C_{8-16}G_X$/water system

In contrast to the $C_{8-10}G_X$/water and $C_{12-14}G_X$/water systems the phase diagram for the $C_{8-16}G_X$/water system is to our knowledge not described in the literature. For this reason the phase diagram was estimated using two different methods. The first method was the visual observation of a solution with a known amount of surfactant during heating. Cloud points were taken at the temperature at which the first sign of cloudiness

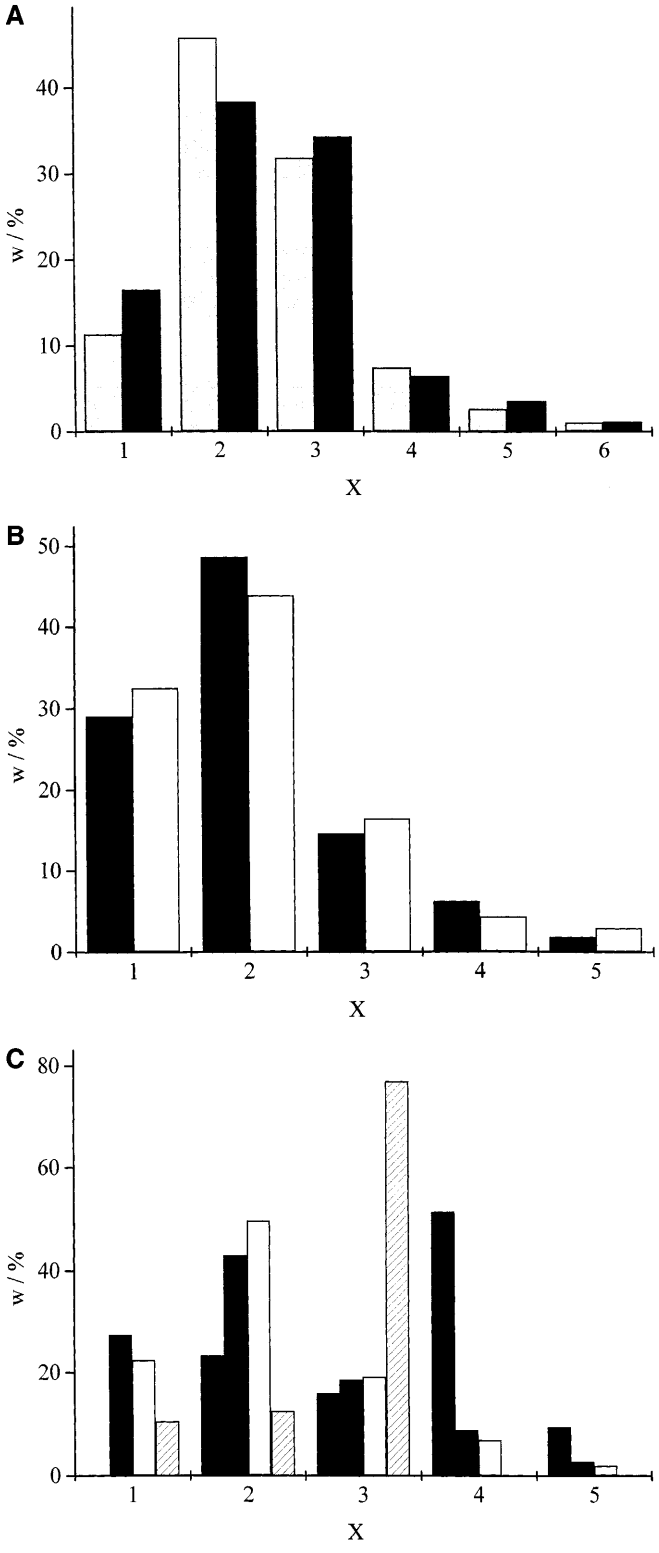

Fig. 2 Distribution of the number of the glucose groups, *X*, as function of the *n*-alkyl chain length, *Y*, (*light grey*: C_8, *dark grey*: C_{10}, *black*: C_{12}, *white*: C_{14} and *patterned*: C_{16}) obtained by atmospheric pressure ionisation – mass spectroscopy for **A** $C_{8-10}G_X$, **B** $C_{12-14}G_X$ and **C** $C_{8-16}G_X$

appeared in the heating mode. The second method was a rheological method. It is well known that the shear viscosity, η, of mixed liquids exhibits divergent anomalies approaching the phase boundary [27]. Other rheological properties, such as the shear moduli, show similar anomalies near the phase boundaries [12]. The shear moduli were measured during an oscillation experiment as a function of temperature [12, 18].

The experimentally determined phase separation temperatures are depicted as a function of surfactant concentration for the $C_{8-16}G_X$/water system in Fig. 3. The system shows an LCST (lower critical solution temperature) behaviour, similar to the $C_{12-14}G_X$/water system [5]. Below the curve, the samples are transparent and homogeneous; above the curve, droplets begin to appear, which make the solution cloudy. In comparison to the $C_{12-14}G_X$/water system the demixing region in the $C_{8-16}G_X$/water system is larger and is shifted to lower temperatures; however, the miscibility gap for the $C_{8-16}G_X$/water system is smaller than in the $C_{12}G_1$/water system [14], although the weight-average chain length for the technical grade surfactant (Table 1) is higher than for $C_{12}G_1$. This indicates the influence of the head groups on the demixing behaviour. At surfactant concentrations higher than 55 wt% liquid-crystalline phases with a lamellar structure appear [18].

Rotation experiments

The rotation experiments were carried out at constant stress. Figure 4 shows the viscosities, which are equal to the slope of the flow curve, at constant temperature. For the $C_{8-10}G_X$/water system the viscosity increases very slowly with increasing surfactant concentration. This system behaves as a Newtonian fluid over a wide shear-rate range up to very high concentrations. These findings

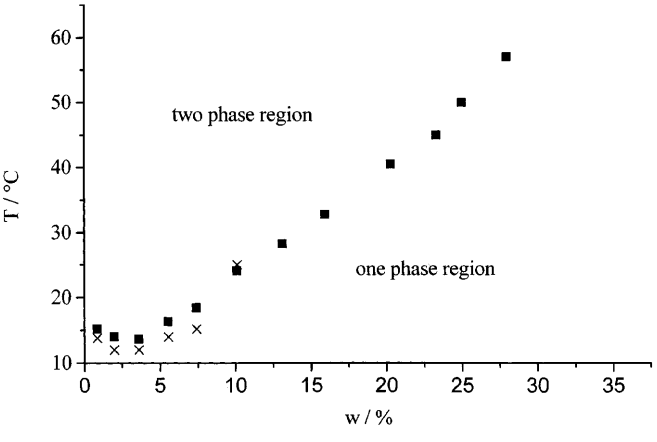

Fig. 3 Phase diagram for the $C_{8-16}G_X$/water system detected by rheological experiments (*crosses*) and visual observations (*squares*)

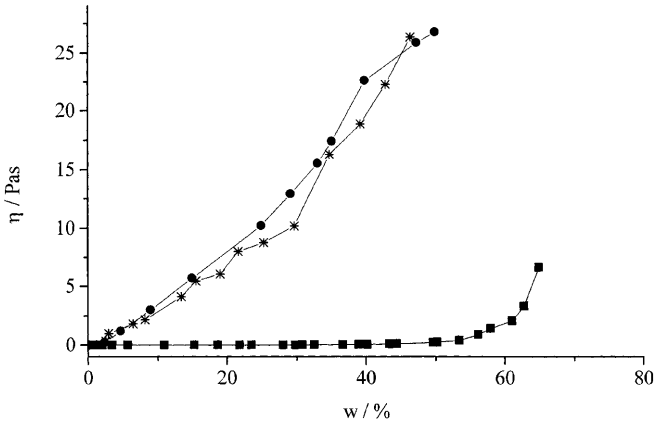

Fig. 4 Plot of viscosity, η, obtained by rotation experiments, versus surfactant concentration expressed as mass fraction at 20 °C for the following systems: $C_{8-10}G_X$/water (*squares*), $C_{12-14}G_X$/water (*circles*) and $C_{8-16}G_X$/water (*stars*)

are identical to the results of Platz et al. [5]. Deviations from Newtonian fluid behavior occur near the boundary to the liquid-crystalline phases. The flow curves in this concentration range follow a power law [18], indicating shear-thickening in the $C_{8-10}G_1$/water system.

In contrast to the $C_{8-10}G_X$/water system the two other systems show an approximately linear increase in the viscosities with surfactant concentration, and the viscosities are much higher. From the relatively high viscosity of these systems, it can be deduced that the micellar aggregates in these solutions organize themselves into some kind of supermolecular network. Both surfactant systems have a similar weight-average chain length (Table 1), where the surfactant $C_{12-14}G_X$ has a slightly higher average chain length. This results in a slightly higher viscosity at constant concentration in comparison to the $C_{8-16}G_X$/water system. Within the experimental shear-rate range these systems also show Newtonian fluid behaviour. Rodlike micelles can be aligned in a flow direction in a shear field and consequently give rise to a dependence of the viscosity on shear rate [1, 28, 29]. Furthermore, viscosity measurements should show clearly the beginning of overlaps of the rods. These rods can no longer rotate freely in a shear field because of their strong mutual hindrance, therefore the viscosity has to increase rapidly for concentrations above the overlap concentration. The overlap concentration coincides roughly with the surfactant concentration where the rods have their maximum length [28]. The data given in Fig. 4 do not show a rapid rise for the $C_{8-10}G_X$/water system. Platz et al. [5] interpreted their rheological results, obtained for the $C_{12-14}G_X$ system, of especially large viscosities in the diluted concentration range, as being due to the steric hindrance to the shearing of rod micelles which are formed even at very low concentrations and overlap. In our experiment these systems show Newtonian flow behaviour over a wide shear-rate range. Generally, one finds spherical micelles before the cubic phase, rodlike micelles before the hexagonal phase and disklike micelles before the lamellar phase. In the $C_{12-14}G_X$/water [5] and $C_{8-16}G_X$/water systems no hexagonal phases have been observed until now. The shear orientation of a micellar hexagonal liquid-crystalline phase was investigated by small-angle neutron scattering [30]. The type of micelle is determined by the surface area that a surfactant molecule requires at the micellar interface. From theoretical predictions [31] based on a detailed micellar formation model, these systems should favour the formation of spherical bilayer vesicle structures. In summary, the surfactant does not form rodlike micelles in contact with water.

The viscosity is highly sensitive to changes in temperature. The temperature dependence of the viscosity follows the Arrhenius law (Andrade equation):

$$\eta = A \exp\left(\frac{E_a}{RT}\right) \quad , \tag{4}$$

where A is the pre-expotential factor and E_a the shear activation energy. The shear activation energies as a function of surfactant concentration are shown in Fig. 5. At low surfactant concentration the shear activation energy increases rapidly with the surfactant concentration for the $C_{12-14}G_X$/water and $C_{8-16}G_X$/water systems and reaches a nearly constant value at approximately 10 wt%. For the other three systems ($C_{8-10}G_X$/water, C_8G_1/water and $C_{10}G_1$/water) at low concentration the shear activation energy lies at very low

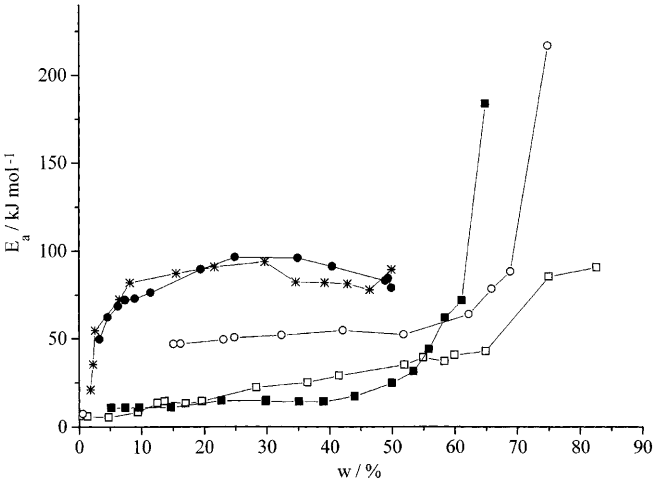

Fig. 5 Plot of shear activation energy E_a, obtained by rotation experiments at different temperatures and Eq. (4), versus surfactant concentration expressed as mass fraction for the following systems: $C_{8-10}G_X$/water (*filled squares*), $C_{12-14}G_X$/water (*filled circles*), $C_{8-16}G_X$/water (*stars*), C_8G_1/water (*open squares*) and $C_{10}G_1$/water (*open circles*)

values: lower than the values for pure water. A possible explanation may be that the surfactant molecules destroy the special structure of water. In the semidiluted concentration range the energy increases slightly with the surfactant weight fraction. The temperature dependence of the mutual and the self-diffusion coefficients in the $C_{10}G_1$/water system obtained by dynamic light scattering and PFG-NMR also shows only a small dependence on surfactant concentration in the semidilute region [18]. Moreover, the self-diffusion coefficients depend only slightly on the surfactant concentration for the C_8G_1/water [10], C_9G_1/water [10] and $C_{10}G_1$/water [10, 18] systems. The reason for this is the fact that the number of available surfactant diffusion paths increases as the junctions of the network come closer to each other with increasing concentration [10]. As the surfactant concentration is increased, the microstructure evolves continuously into a situation of bicontinuous micelles. Such a bicontinuous structure can be imagined to be a randomly connected bilayer network [32]. The formation of such a network explains the nearly constant diffusion coefficients, although the viscosity increased with increasing surfactant concentration (Figs. 4, 5). The temperature dependence of the transport properties (mutual diffusion, self-diffusion and viscosity, Fig. 5) is very similar, indicating that the network should be stable in the temperature range considered. The rapid rise in the energy values over 60 wt% is due to the liquid-crystalline phase which occurs in this concentration range [5, 8–12]. For the $C_{10}G_1$/water system the isotropic micellar solution splits into two phases [13, 14, 26] differing in the surfactant concentration. The activation energy E_a increases with increasing alkyl chain length at a given surfactant concentration in the semidiluted region. Comparison of the water-containing C_8G_1 and $C_{8-10}G_X$ systems demonstrates the influence of the head group on the rheological properties. The general behaviour of the shear activation energy as a function of surfactant concentration (Fig. 5) is different to the behaviour of the tetradecylpyridinium-*n*-heptanesulfonate system [33], where rodlike micelles are present. The activation-energy curve for viscous flow passes through a maximum value at about 40 mM [33]. The maximum is probably due to the fact that both the ratio of the long and short axes of the rod and the long axes self reach a maximum value [33]. This can be interpreted as an additional hint that no rodlike micelles will be formed in the systems studied.

Oscillation experiments

The viscoelasticity of the samples was determined by plotting the storage and loss moduli against the frequency of the applied oscillations. A representative experimental result is shown in Fig. 6. The storage modulus, G', and the loss modulus, G'', are plotted against the angular frequency ω for a solution of $C_{12-14}G_X$ in water at $w = 0.045$. The dynamic characteristic of this solution is very similar to the dynamical behaviour of the pure surfactant solutions [12, 18]. The rheological parameters τ and G_0 were fitted to the experimental G'' values according to Eq. (2). Using these parameters (τ and G_0) G' was predicted by applying Eq. (1).

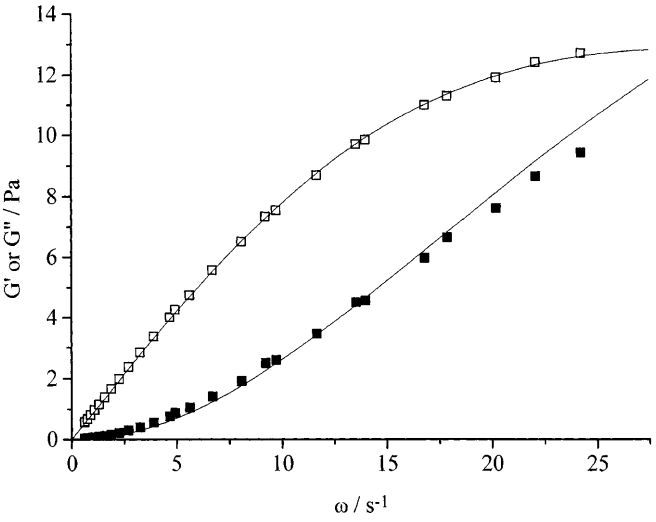

Fig. 6 Analysis of the rheological oscillation experiment according to the Maxwell model (Eqs. 1, 2) for the $C_{12-14}G_X$/water system at 20 °C. An example (surfactant weight fraction $w = 4.5\%$) for the fit of the experimental loss modulus, G'', (*open squares*) using Eq. (2) is shown. The experimental storage modulus, G', (*solid squares*) is predicted by the Maxwell model, Eq. (1), using $G_0 = 25.7$ Pa and $\tau = 33.6$ ms

Figure 6 illustrates that the experimental points coincide nicely with the ideal solid curve in the low-frequency range. This curve suggests that the Maxwell model (Eqs. 1, 2) describes the linear viscoelastic behaviour of the mixtures over the low-frequency range. The corresponding relaxation processes are characterized by one single relaxation time. Modelling of the rheogram using the "wedge-box" model [34] over the whole frequency range fails. The modelled spectrum of relaxation times is of the "wedge-box" type where the "wedge" portion is located at the short-time scale of relaxation times and the "box" part covers the long-time scale [34]. Furthermore, it becomes obvious that $G'(\omega)$ and $G''(\omega)$ of the micellar solutions are determined by the stationary values of η_0 and τ according to the theoretical predictions of Eqs. (1 and 2); therefore, the dynamical properties of the solution at different concentrations can be fitted by a master curve.

In this concentration region the stress relaxation time coincides with the slow relaxation time of the kinetic processes that are present in micellar solutions. Figure 7A depicts τ as a function of the surfactant

concentration. The relaxation times were obtained by fitting the experimental G'' data to Eq. (2). In general, an increase in surfactant concentration produces a decrease in the characteristic relaxation time, similar to the poly(ethylene glycol) nonylphenylether/water system [35]. For all systems, except the $C_{8-10}G_X$/water system, the τ values run through a maximum value at low surfactant content. Platz et al. [5] also found a maximum in the structure relaxation times as a function of surfactant weight fraction for the technical grade $C_{12-14}G_X$/water system. The maximum is located nearly at the same position. In the case of $C_{8-10}G_X$/water it was not possible to determine these values [5]. They figured out that the concentration, where τ runs through a maximum, corresponds roughly to the minimum of the miscibility gap arising in the $C_{12-14}G_X$/water system. For the pure surfactant systems we did not find a similar relation [12]. The maximum for the $C_{10}G_1$/water system occurs clearly at higher concentrations than the minimum of the cloud-point curve. The C_8G_1/water system does not show a two-phase region at low surfactant concentration. According to the Lequeux model [36], the reptation process is speeded up by the formation of crosslinks and therefore the terminal time is reduced. Generally, increasing the carbon number of the tail leads to a shorter relaxation time. The same effect was described by Hoffman et al. [37] for ionic surfactant systems. This is because in the kinetically controlled region the breaking and forming of the micelles depends very much on the chain length of the surfactant. At high surfactant concentrations τ approaches the same values, independent of the chain length and the head group of the surfactant.

The shear moduli, G_0, which are obtained by the Maxwell model, are plotted as a function of sugar surfactant concentration in Fig. 7B. In discussions on the microscopic aspect of viscoelasticity the plateau value, G_0, is usually related to the number of crosslinks in the system; hence, G_0 depends upon the number density of the elastically effective chains. The decreasing of G_0 at high surfactant concentrations (Fig. 7B) for the $C_{10}G_1$/water system indicates structural changes in the system. Inspection of the phase diagrams shows that the liquid-crystalline phases appear in this concentration range [12]. In addition, the C_8G_1/water and $C_{8-10}G_X$/water systems and the $C_{12-14}G_X$/water and $C_{8-16}G_X$/water systems behave very similarly. This indicates clearly that the dynamical properties are much more dependent on the chain length than on the number of glucose units.

The zero-shear viscosity results calculated from the Maxwell model are shown in Fig. 7C. The η_0 values increase with increasing surfactant concentration for all the systems studied. The maximum in η_0 for the C_8G_1/water system is situated at a surfactant concentration of nearly 0.6 and is related to the transition into a liquid-

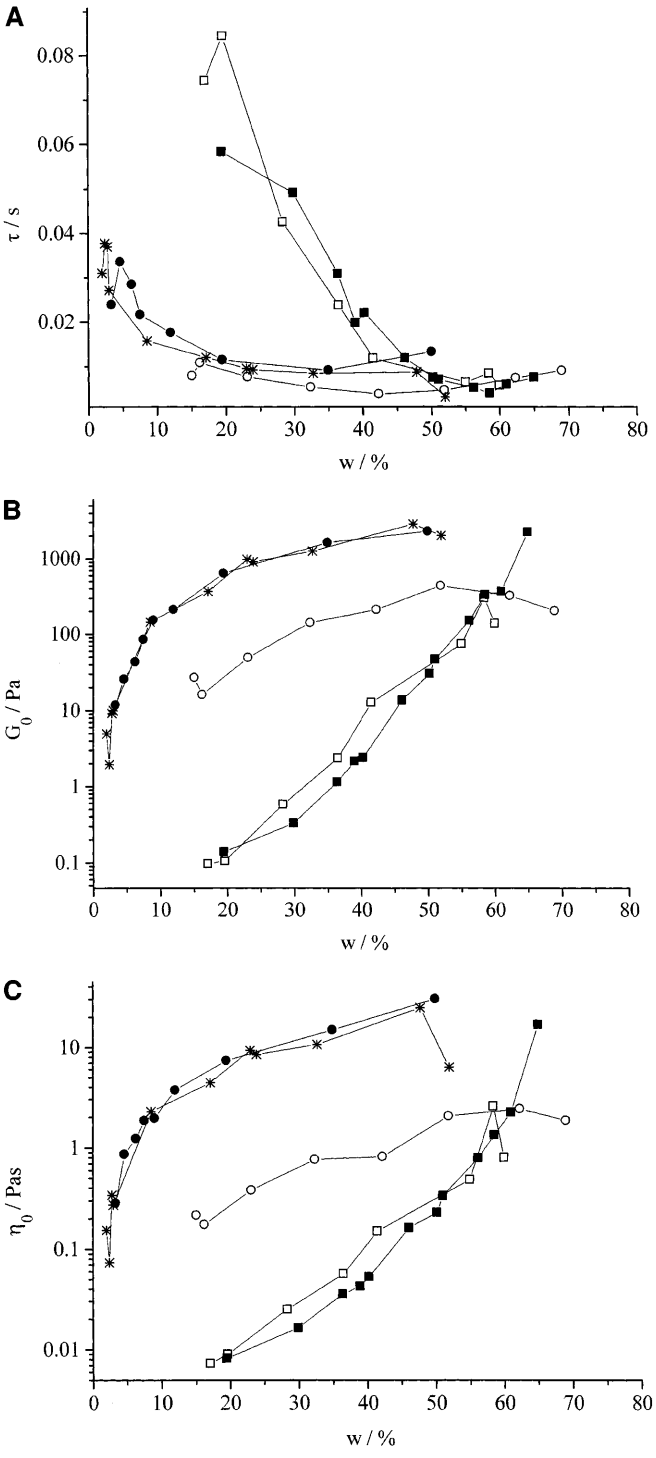

Fig. 7 Rheological parameters **A** structure relaxation time, τ, **B** zero-shear modulus, G_0 and **C** zero-shear viscosity, η_0, obtained by the Maxwell model (Eqs. 1, 2) for $C_{8-10}G_X$/water (*solid squares*), $C_{12-14}G_X$/water (*solid circles*), $C_{8-16}G_X$/water (*stars*), C_8G_1/water [12] (*open squares*) and $C_{10}G_1$/water [12] (*open circles*) as functions of the surfactant weight fraction

crystalline phase. This behaviour is different from the behaviour in the ethanediyl-α,ω – bis(dodecyldi-methylammonium bromide)/water system, where the maximum of η_0 as function of surfactant concentration is related to the maximum in micellar length when the surfactant volume fraction is varied [38].

Investigation of G', G'' and $|\eta^*|$ as a function of temperature permits us to determine the phase-transition temperature for a given surfactant solution [12]. The measurements were performed as a function of temperature at fixed amplitude. $|\eta^*|$, G' and G'' are shown as a function of temperature for the $C_{12-14}G_X$/water system in Fig. 8.

A large number of papers have been published on shear-flow effects in various fluids undergoing some phase transition. Onuki [39] gives a review of the theories and experiments related to this field. Recently [12, 18] it was shown for the C_8G_1/water system, that oscillation experiments are suitable for phase-transition determination from an isotropic to a liquid-crystalline phase. Due to the large difference in the complex moduli between an isotropic and a liquid-crystalline phase both moduli change significantly on passing the phase boundary. In comparison to this phase transition the rheological properties differ only slightly during the transition between a homogeneous solution and a demixed system. Figure 8 depicts the corresponding quantities as functions of temperature for the $C_{12-14}G_X$/water system at $w = 10$ wt%. The $|\eta^*|$ and G' values decrease continuously with increasing temperature. No phase separation can be detected. In contrast to these quantities G'' exhibits a significant discontinuity at 35 °C. This discontinuity corresponds to the phase-separation temperature, according to the phase diagram, but the temperature is at a slightly lower temperature than the literature value [5]. In the two-phase region above 35 °C G' increases with increasing temperature. By constructing the Cole–Cole plot from the experimental data the phase separation is clearly indicated [40].

The $C_{8-10}G_X$/water system displays a phase transition from an isotropic solution to a lamellar liquid-crystalline phase at lower temperatures [5]. The dynamical properties exhibited during this phase transition for the $C_{8-10}G_X$/water system at 48.7 wt% surfactant are demonstrated in Fig. 9. At low temperatures the lamellar phase with a high viscosity is present. An increase in temperature leads to a transition region where an isotropic solution coexists with a liquid-crystalline phase. At about 14 °C only the isotropic liquid is stable and the rheological quantities decrease continuously with increasing temperature according to the Arrhenius law (Eq. 4).

Synergetic effects

For a mixture of surfactants to exhibit synergism in its interfacial properties, the different types of interface-active molecules in the mixture must attract each other. When synergy exists, a mixture of two surfactants exhibits better interfacial properties than either surfactant by itself. The requirements, in quantitative terms, for the existence of synergy in mixtures of surfactants have been elucidated for several interfacial phenomena [41, 42]. The viscosities obtained by rotation experiments as a function of the amount of surfactant added to a $C_{8-10}G_X$ solution with a concentration of 15.3 wt% are shown in Fig. 10A. On adding an anionic surfactant, for instance SDS, to a $C_{8-10}G_X$ solution, the viscosity increases much more with increasing total surfactant concentration than in the case where $C_{8-10}G_X$ was added. Synergism in microemulsion solubilization has been reported for a nonionic–anionic

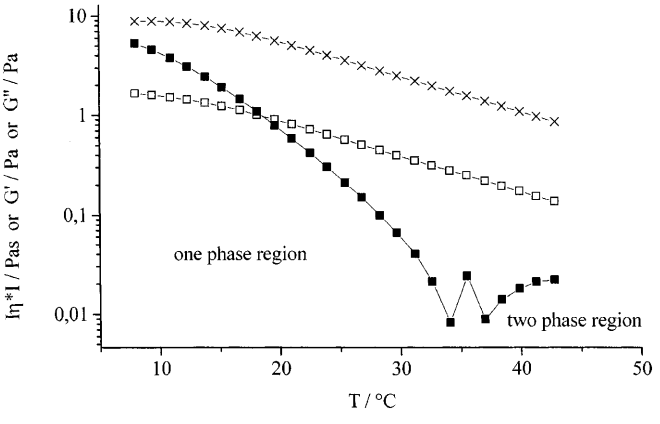

Fig. 8 Dynamical properties (viscosity [*open squares*], loss modulus [*crosses*] and storage modulus [*solid squares*]) plotted versus temperature for the $C_{12-14}G_X$/water system ($w = 10\%$) measured at 1mNm and 1 Hz

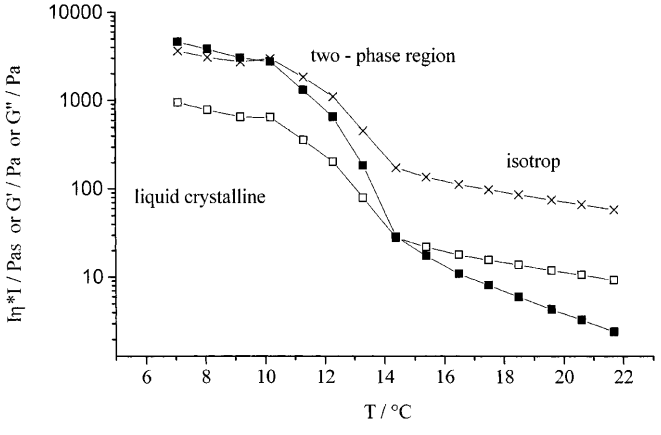

Fig. 9 Dynamical properties (viscosity [*open squares*], loss modulus [*crosses*] and storage modulus [*solid squares*]) plotted versus temperature for the $C_{8-10}G_X$/water system ($w = 48.7\%$) measured at 1mNm and 1 Hz

system designed for pharmaceutical applications, using mixtures of sodium bis(2-ethylhexyl)sulfosuccinate and sorbitan laureate in different proportions [43, 44]. A possible explanation may be that incorporation of SDS molecules into micelles formed for $C_{8-10}G_X$ leads to a decrease in the repulsive interaction between the charged head groups of the SDS molecule. The formation of mixed micelles permits more growth of the micelles connected with a higher viscosity. Adding the cationic surfactant DMAB to a sugar surfactant solution results in a lower viscosity compared to a sugar surfactant solution at the same total surfactant concentration (Fig. 10A). These findings indicate that it is difficult to incorporate DMAB into a micelle based on nonionic surfactant or that the aggregation shape is changed. The change in viscosity upon adding nonionic surfactants depends on the structure of the surfactant (Igepal or Brij35). Nonionics, which have minimal intermolecular interactions, should have, by comparison, the lowest synergism of all mixtures [21]. A recent paper [45] reports strong synergism in nonionic surfactant mixtures and provides evidence for two different synergism mechanisms. Mixtures of a highly oil soluble surfactant and a highly water soluble surfactant achieved the maximum water solubilization, evidently overcoming the expected partitioning of the two surfactant components into the oil and water phases and enhancing their partitioning to the interface [45].

Anionic surfactants show a very important effect, and for this reason we studied the influence of the chain length of the hydrophobic tail on the rheological behaviour. Figure 10B illustrates the viscosities measured by rotation experiments as functions of the amount of anionic surfactants with different tail lengths. Increasing the tail length leads to a stronger hydrophobic character of the surfactant and to a decrease in the solubility in water. For this reason only 10 wt% SOS could be added without precipitation of the surfactant. At a certain concentration of the second surfactant the viscosity increases rapidly by several orders of magnitude. This concentration shifts to lower values if the chain length of the hydrophobic tail increases. Thus the data presented indicate that the second surfactant may influence the rheological properties of the solution in different ways. This provides a means to adjust their properties and to develop phases with the desired rheological behaviour.

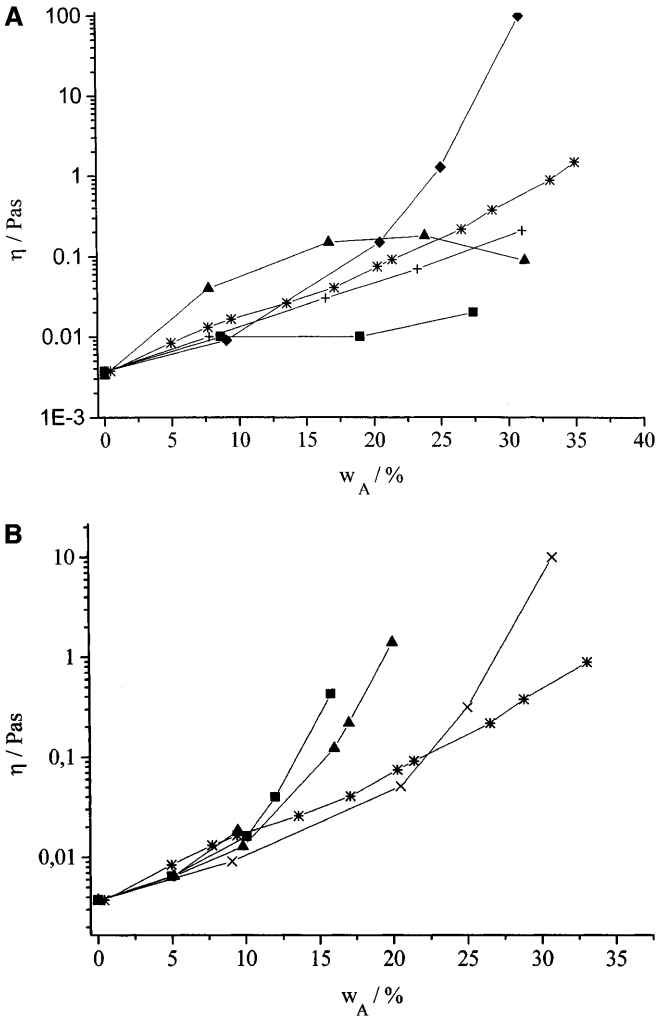

Fig. 10A, B Visocities obtained by rotation experiments plotted versus the amount of surfactant w_A added to a 15.3 wt% $C_{8-10}G_X$ solution at 20 °C. **A** The surfactants added are sodium dodecylsulfate (*SDS*) (*diamonds*), dodecyl trimethylammonium bromide (*squares*), Brij35 (*crosses*), Igepal (*triangles*), or $C_{8-10}G_X$ (*stars*) **B** The surfactants added are sodium tetradecylsulfate (*triangles*), sodium hexadecylsulfate (*squares*), sodium octadecylsulfate (*circles*), SDS (*crosses*), or $C_{8-10}G_X$ (*stars*)

Conclusion

The experimental results demonstrate that the degree of glucosidation as well as the *n*-alkyl chain length is an important parameter for controlling the rheological parameters, but the chain length is the dominating influence on these properties.

In the semidiluted concentration range the linear viscoelastic response is consistent with that of a viscoelastic liquid and can be successfully described by the Maxwell model in the low-frequency range. The viscosities of the mixtures show an Arrhenius-like dependence on temperature, whereas the shear activation energy is only a slight function of surfactant concentration.

When two phases have very different flow properties (for instance isotropic solution to liquid-crystalline phase), there arises a sudden rise or drop near the phase-transition line of the rheological properties leading to a good possibility to detect phase-transition phenomena. Oscillation experiments conducted over a range of temperatures appear to be sensitive tools in the

study of the phase transformation of surfactant solutions.

One of the keys to the successful use of mixtures in commercial formulations is to take advantage of synergy. The phenomenon has, however, considerable potential for technical applications where it is necessary to control the flow behaviour of aqueous surfactants solutions. Using anionic surfactants leads to an increase in the viscosity, while applying a cationic surfactant decreases the viscosity. The behaviour of a nonionic surfactant depends on the structure of the surfactant.

Acknowledgements The financial support of the "Deutsche Forschungsgemeinschaft" and of the state of Saxona is gratefully acknowledged. A. Schreiber and W. Engewald, University of Leipzig, Institute of Analytical Chemistry, are gratefully acknowledged for carrying out the API-MS experiments. The authors thank Henkel, Düsseldorf for the gift of technical grade alkylpolyglucosides.

References

1. Hoffmann H, Ulbricht W (1997) In: Esumi K (ed) Structure–performance relationship in surfactants. Dekker, New York, pp 285–324
2. Hill K, von Rybinski W, Stoll G (1997) Alkyl polyglucosides. VCH, Weinheim
3. von Rybinski W, Hill K (1998) Angew Chem 110:1394
4. von Rybinski W (1996) Curr Opin Colloid Interface Sci 1:587
5. Platz G, Pölike J, Thuning C, Hoffmann R, Nickel D, von Rybinski W (1995) Langmuir 11:4250
6. Fukada K, Södermann O, Lindmann B, Shinoda K (1993) Langmuir 9:2921
7. Balzer D (1993) Langmuir 9:3375
8. Nillsson F, Södermann O, Johansson I (1996) Langmuir 12:902
9. Sakya P, Seddon JM, Templer RH (1994) J Phys II 4:1311
10. Nilsson F, Söderman O, Hansson P, Johansson I (1998) Langmuir 14:4050
11. Loewenstein A, Igner D (1993) Liq Cryst 13:531
12. Häntzschel D, Schulte J, Enders S, Quitzsch K (1999) Phys Chem Chem Phys 1:895
13. Kahl H, Quitzsch K, Stenby EH (1997) Fluid Phase Equilib 139:295
14. Ryan LD, Kaler EW (1997) Langmuir 13:5222
15. La Mesa C, Bonincontro A, Sesta B (1993) Colloid Polym Sci 271:1165
16. Förster T, Guckenbiehl B, Hensen H, von Rybinski W (1996) Prog Colloid Polym Sci 101:105
17. Shchipunov YA, Shumilina EV, Hoffmann H (1998) Colloid Polym Sci 276:368
18. Schulte J (1998) Thesis. University of Leipzig
19. Platz G, Thuning C, Pölike J, Kirchhoff W, Nickel D (1994) Colloids Surf A 88:113
20. Rosen MJ (1994) Prog Colloid Polym Sci 95:39
21. Rosen MJ (1989) Surfactants and interfacial phenomena. Wiley, New York, pp 398–402
22. Ferry JD (1980) Viscoelastic properties of polymers. Wiley, New York
23. Tschoegl NW (1989) The phenomenological theory of linear viscoelastic behavior. Springer, Berlin, Heidelberg, New York
24. DeGrip WJ, Bovee-Geurts PHM (1979) Chem Phys Lipids 23:321
25. Lafosse M, Marinier P, Joseph B, Dreux M (1992) J Chromatogr 623:277
26. Kahl H (1996) Thesis. University of Leipzig
27. Sengers JV (1971) In: Green MS (ed) Critical phenomena. Academic Press, New York, pp 112–154
28. Hoffmann H (1984) Ber Bunsenges Phys Chem 88:1078
29. Wang SQ (1992) Colloid Polym Sci 270:1130
30. Richterling W, Schmidt G, Lindner P (1996) Colloid Polym Sci 274:85
31. Enders S, Häntzschel D (1998) Fluid Phase Equilib 153:1
32. Strey R, Jahn W, Porte G, Bassereau P (1990) Langmuir 6:1635
33. Hoffmann H, Rehage H, Platz G, Schorr W, Thurn H, Ulbricht W (1982) Colloid Polym Sci 260:1042
34. Manero O, Soltero JFA, Puig JE, Gonzalez-Romero VM (1997) Colloid Polym Sci 275:979
35. Cordobes F, Munoz J, Gallegos C (1997) J Colloid Interface Sci 187:401
36. Lequeux F (1992) Europhys Lett 19:675
37. Hoffmann H, Löbl H, Rehage H, Wunderlich I (1985) Tenside Deterg 22:290
38. Kern F, Lequeux F, Zana R, Candau SJ (1994) Langmuir 10:1714
39. Onuki A (1997) J Phys Condens Matter 9:6119
40. Ajji A, Choplin L, Prud'Homme RE (1988) J Polym Sci Part B Polym Phys 26:2279
41. Hua XY, Rosen MJ (1982) J Colloid Interface Sci 90:212
42. Hua XY, Rosen MJ (1988) J Colloid Interface Sci 125:730
43. Johnson KA, Shah DO (1985) J Colloid Interface Sci 107:269
44. Johnson KA, Shah DO (1986) In: Mittal KL, Bothorel P (eds) Surfactants in solutions, Vol 6. Plenum, New York, pp 120
45. Huibers PDT, Shah DO (1997) Langmuir 13:5762